

## Theory of Directed Nucleation of Strained Islands on Patterned Substrates

Hao Hu,<sup>1,2</sup> H. J. Gao,<sup>1</sup> and Feng Liu<sup>2,\*</sup>

<sup>1</sup>*Institute of Physics, Chinese Academy of Science, Beijing 100190, China*

<sup>2</sup>*Department of Materials Science and Engineering, University of Utah, Salt Lake City, Utah 84112, USA*

(Received 23 April 2008; published 20 November 2008)

We develop a theoretical model to elucidate the nucleation of strained islands on patterned substrates. We show that island nucleation is directed to the preferred sites by a much lower energy barrier and smaller critical size. Strain relaxation directs island nucleation to the bottom of a pit rather than the top of a ridge as commonly perceived, while large surface energy anisotropy favors nucleation at both places. The theory explains some puzzling experimental results and provides useful guidelines for future experiments.

DOI: 10.1103/PhysRevLett.101.216102

PACS numbers: 68.35.Gy, 68.35.Md, 81.10.Aj

Understanding the nucleation process, a critical kinetic step in material growth and phase transitions, is not only of fundamental interest but also has significant technological implications. For example, heteroepitaxial growth of strained islands offers an attractive route to the fabrication of quantum dots (QDs) [1]. To improve the uniformity of QDs, one strategy is to convert the otherwise “stochastic” nucleation process into a “deterministic” one by directing nucleation to the predefined surface sites via surface engineering. This has been achieved by generating a surface strain field from buried dislocation networks [2] or strained islands [3], and by using steps [4] or patterned topographic surface features [5–15].

Recent efforts have focused on using lithographically patterned substrates [5–15], producing QD arrays with some of the highest spatial and size uniformity. On a flat substrate, island nucleation is inherently a stochastic process, rendering a random spatial distribution that also broadens the island size distribution. The key is to direct island nucleation to the predesigned patterning sites, which not only induces high spatial order of islands but also improves their size uniformity. This approach appears intuitively obvious, but the underlying physical mechanism remains poorly understood.

Experiments to date have been done in a trial-and-error manner. In particular, different patterns, e.g., mounds and ridges [5–12] versus voids and pits [13–15], have been used without *a priori* knowledge of which pattern works best under which conditions. Experimental results are not adequately explained. In this Letter, we develop a theoretical model to elucidate island nucleation on patterned substrates answering two critical questions: (1) How do island nucleation barrier and critical nucleus size on a patterned substrate differ from those on a flat substrate? (2) What are the physical parameters that control the preferred sites for nucleation?

The theory of strained island nucleation on a flat substrate has been well established [16–19]. In general, the criticality of nucleation is determined by the competition between strain energy and surface energy. There can be

also an edge energy term [17], but it is usually small; for instance, it is negligible for the Ge island grown on Si [19]. Here, we formulate a calculation of island nucleation barrier and critical size on patterned substrates.

We consider first a 2D model of the island on a sawtooth surface pattern, as shown in Fig. 1(a). The surface pattern is assumed to have a constant slope of angle  $\varphi$ , which may or may not be a facet. The island is bound by two facets of contact angle  $\theta \geq \varphi$  with a base dimension  $2l$ . The island strain relaxation energy, i.e., the strain energy difference between the island and the uniformly strained film, is calculated using the Green’s function method within the shallow-angle approximation [16]:

$$E_e = -\frac{\sigma^2}{2} \iint dx dx' \chi(x-x') \partial_i t(x) \partial_j t(x'). \quad (1)$$

$\sigma$  is the bulk stress in the island,  $x$  and  $x'$  denote the

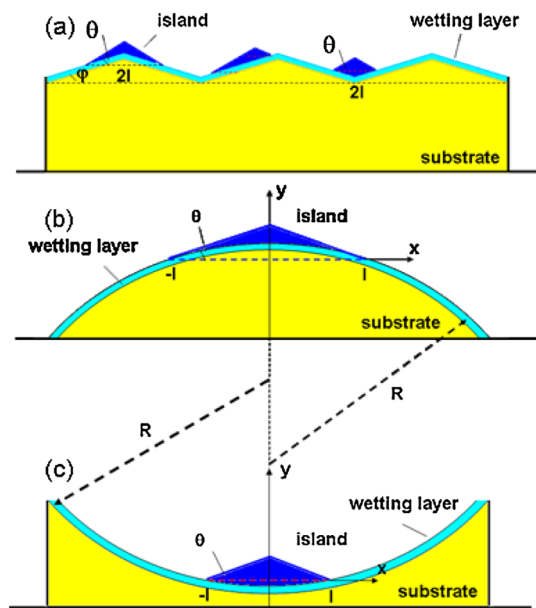


FIG. 1 (color online). Schematic illustration of island nucleation on patterned substrates. (a) On a sawtooth pattern; (b) on the apex of a concave surface; (c) in the valley of a convex surface.

position along the surface,  $\chi$  is the Green's function relating the displacement at  $x'$  induced by a force at  $x$ , and  $t(x)$  is the island thickness function.

Figure 2 illustrates the type of elastic forces (monopoles vs dipoles) induced in a strained film by film thickness variation and surface waviness. For constant film thickness on a flat surface [Fig. 2(a)], no force is induced (no strain relaxation). For changing film thickness on a flat surface [Fig. 2(b)], forces are induced only on the film surface, leading to monopole-monopole interaction. For constant film thickness on a wavy surface [Fig. 2(c)], forces of the same magnitude but opposing directions are induced at both the film surface and the film-substrate interface, leading to dipole-dipole interaction. For changing film thickness on a wavy substrate [Fig. 2(d)], both force monopoles and dipoles are present. Since the monopole-monopole interaction energy scales as  $\ln(L)$ , where  $L$  is the lateral dimension of the film (e.g., the size of an island), and the dipole-dipole interaction energy scales as  $1/L^3$ , to the first-order approximation, we will include only the force monopoles induced by the film thickness variation, i.e.,  $\partial_i t(x)$  in Eq. (1), and neglect the force dipoles induced by surface waviness.

Solving Eq. (1), we obtain

$$E_e = -\varepsilon_0 S (\tan\theta - \tan\varphi). \quad (2)$$

$\varepsilon_0 = (2 \ln 2) \sigma^2 (1 - \nu^2) / \pi Y$  is the scaled elastic energy density,  $\nu$  is Poisson ratio, and  $Y$  is Young's modulus.  $S = l^2 (\tan\theta - \tan\varphi)$  is the island area (size). In deriving Eq. (2) we consider that island can locate either on the top of the apex [the left island in Fig. 1(a)] or at the bottom of the valley [the right island in Fig. 1(a)] sitting centered at the corner. For a given  $\theta$ ,  $\varphi$  may vary as  $-\theta \leq \varphi \leq \theta$ , being positive when island is on the apex and negative in the valley.

The extra surface energy created by the island is

$$E_s = 2l(\gamma_f \sec\theta - \gamma_w \sec\varphi) = 2\Gamma S^{1/2} (\tan\theta - \tan\varphi)^{1/2}. \quad (3)$$

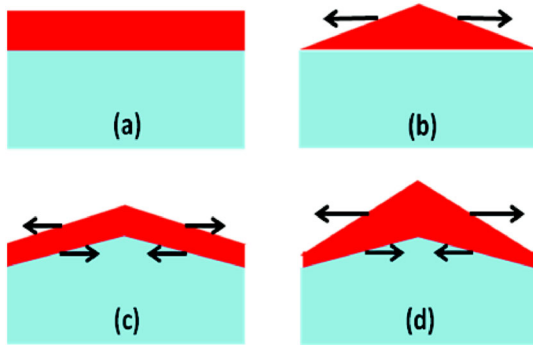


FIG. 2 (color online). Schematic illustration of elastic forces generated in a strained film. (a) Constant film thickness on a flat surface; (b) varying thickness on a flat surface; (c) constant thickness on a wavy surface; (d) varying thickness on a wavy surface.

$\Gamma = (\gamma_f \sec\theta - \gamma_w \sec\varphi)(\tan\theta - \tan\varphi)^{-1}$ ;  $\gamma_f$  and  $\gamma_w$  are surface energy of island facet and wetting layer, respectively. The total island formation energy is then

$$E = E_e + E_s = -\varepsilon_0 S (\tan\theta - \tan\varphi) + 2\Gamma S^{1/2} (\tan\theta - \tan\varphi)^{1/2}. \quad (4)$$

The strain relaxation (the first negative term) lowers the energy favoring island formation, while the surface creation (the second positive term) increases the energy preempting island formation; the competition of the two defines a critical island size ( $S_c$ ) and a energy barrier ( $E_c$ ) as

$$S_c = (\Gamma/\varepsilon_0)^2 (\tan\theta - \tan\varphi)^{-1}; \quad E_c = \Gamma^2/\varepsilon_0. \quad (5)$$

The  $\varphi = 0$  solutions reduce to the critical size and energy barrier on a flat substrate.

The surface energy of the wetting layer ( $\gamma_w$ ) is a function of surface slope, i.e., angle  $\varphi$ . We use a simple generic form of  $\gamma_w = \gamma_0(1 - \alpha \cos(n\varphi))$  [20];  $\alpha$  defines surface energy anisotropy and  $n$  defines the angle of low-energy facets. For the island facet to be the first low-energy facet to appear beyond the flat surface, we have  $\varphi = \theta = 2\pi/n$  and  $\gamma_f = \gamma_0(1 - \alpha)$ . To reveal how critical size and energy barrier on a patterned substrate differ from those on a flat substrate, we examine the dependence of  $S_c$  and  $E_c$  on  $\varphi$  and  $\alpha$ , as shown in Fig. 3. As a typical example, we take  $n = 32$ , representing the growth of the (105)-faceted Ge hut island on Si(001) substrate [19]. For a given  $\varphi$ , it is easy to show  $S_c, E_c \propto (\gamma_0^2/\theta_0)[A - B\alpha]^2$ , where  $A$  and  $B$  are positive constants. Thus, both  $S_c$  and  $E_c$  decrease with the increasing  $\alpha$  (see Fig. 3). This is because for larger  $\alpha$ , the island facet surface energy becomes much lower than the wetting layer surface energy, so that the island can be nucleated much easier with small surface energy cost.

For a given  $\alpha$ , the situation is more complicated. If the surface energy is isotropic ( $\alpha = 0$  or  $\alpha$  is very small), then  $S_c$  and  $E_c$  are smaller in the valley than on the apex so that valleys are preferred nucleation sites. It is because strain relaxation is more effective for islands in the valley than on the apex, as surface energy plays a minimal role for small  $\alpha$ . This may seem at first counterintuitive because hand-waving argument would suggest strain relaxes more when the island is on top of the apex. However, one should realize that strain relaxation is achieved by the film thickness variation, i.e.,  $\partial_i t(x)$  in Eq. (1). If the film had a constant thickness, the strain would be the least relaxed even on a patterned surface [see Fig. 2(c)]. Then it is easy to see in Fig. 1(a) that the island thickness variation is largest when it is in the valley and smallest when it is on the apex. Consequently, island strain is relaxed more in the valley by a bigger geometric factor of  $(\tan\theta + \tan|\varphi|)$  in Eq. (2) than on the apex by a smaller factor  $(\tan\theta - \tan|\varphi|)$ . This is consistent with a recent finite element calculation [14] which showed that the strain energy of a Ge island is lower in the pit than on the flat surface of Si. A

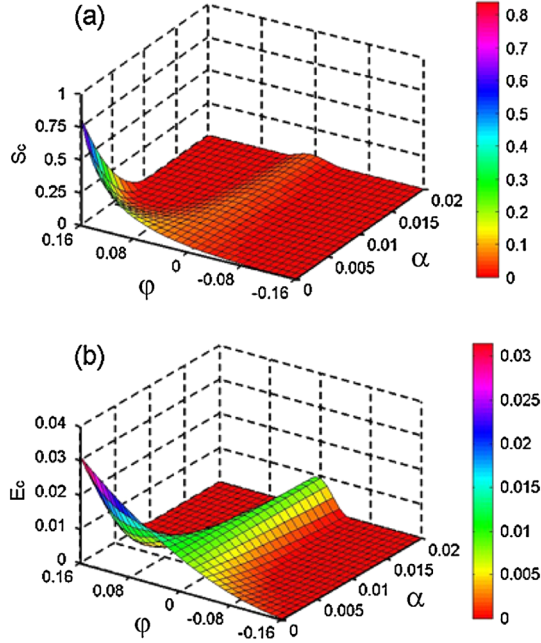


FIG. 3 (color online). Island nucleation critical size (a) and energy barrier (b) as a function of  $\alpha$  and  $\varphi$ . The size is in unit of  $\gamma_0^2/\epsilon_0^2$  and barrier in unit of  $\gamma_0^2/\epsilon_0$ .

similar conclusion is drawn for a continuous strained film on a wavy substrate [21].

If the surface energy is highly anisotropic (large  $\alpha$ ), Fig. 3 shows  $S_c$  and  $E_c$  become smaller both in the valley and on the apex than those on a flat substrate ( $\varphi = 0$ ). For a given  $\alpha$ , the larger the  $\varphi$  is, the smaller  $S_c$  and  $E_c$  will be. This indicates that if surface patterns are steeper, the strained islands are more preferred to nucleate on the apex or in the valley other than in the flat region. However, the underlying mechanism is different in that the island on the apex is only favored by surface energy anisotropy, while the island in the valley is favored by both strain and surface energy effects.

Besides on the apex or in the valley, we also considered island nucleation on a slope (i.e., the sidewalls of a pattern), shown as the middle island in Fig. 1(a). The island formation energy is calculated as

$$E = -\epsilon_0 S \alpha(\theta, \varphi) + \Gamma S^{1/2} \beta(\theta, \varphi), \quad (6)$$

where  $\alpha(\theta, \varphi)$  and  $\beta(\theta, \varphi)$  are complex geometric shape factors and  $\Gamma = [\sec\theta + \sin\varphi \csc(\theta - \varphi)]\gamma_f - [\cos\varphi + \sin\varphi \tan(\theta - \varphi)]\gamma_w$ . Equation (6) has the same form as Eq. (4). Both energy terms on a slope fall in between those on the apex and in the valley, which can be seen by comparing their respective geometries. Consequently, critical size and nucleation barrier on a slope can also be smaller than those on the flat region. A previous analysis shows that island-island interaction may favor island on a slope [22].

The real patterned surface may have a continuously changing surface orientation instead of a constant slope. Therefore, we further consider island nucleation on a

surface with a continuously varying  $\varphi$ , as shown in Figs. 1(b) and 1(c). For simplicity, we assume that the surface has a constant local curvature ( $\kappa = 1/R$ ) underneath the island, and numerically integrate the island total energy. Note that for a given island facet angle, there exists a maximum possible island size, or the surface slope would be larger than the island facet slope on the apex.

Figure 4 compares the island formation energy as a function of size for an island to nucleate on the apex [Fig. 1(b)], in the valley [Fig. 1(c)], and on a flat substrate ( $R \rightarrow \infty$ ). For small  $\alpha$  [Fig. 4(a)], the nucleation barrier is smallest in the valley and highest on the apex. For larger  $\alpha$  [Fig. 4(b)], the barrier on the apex becomes smaller than that on the flat surface. For even larger  $\alpha$  [Fig. 4(c)], the barrier in the valley and on the apex becomes similar; both are much lower than that on the flat surface. These general trends are same as those in Fig. 3.

Although we have presented our theory with a 2D model, a 3D model predicts qualitatively identical behavior [23]. Now, we apply our theoretical predictions to qualitatively explain some interesting and puzzling experiments.

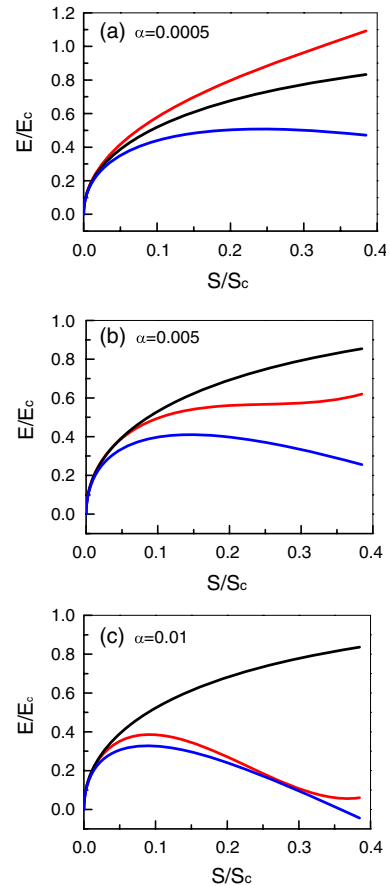


FIG. 4 (color online). Island formation energy ( $E$ ) on a curved surface as a function of island size ( $S$ ), on the apex [red (or gray) line], in the valley [blue (or dark gray) line], and on the flat surface (black line).  $E_c$  and  $S_c$  are energy barrier and critical size on the flat substrate, respectively. We use  $R = 100$  nm and  $2\gamma_0/\epsilon_0 = 100$  nm.

One key prediction is that islands nucleate on a patterned substrate with a smaller critical size and lower energy barrier than those on a flat substrate, and the critical size can be reduced by 1 order of magnitude (see Fig. 4). This is consistent with experimental observations [5–15]. For example, under identical growth conditions, InAs islands are shown to nucleate with a much higher density on top of the patterned GaAs stripes than on the planar surface [9].

The reduced critical size has an important implication for the island growth mechanism: while nucleation mechanism (such as Ge islands grown on Si) may be bypassed on a flat substrate [20] due to too big a critical size (a few thousands of atoms) [19] (the faceted islands form instead via a barrierless transformation from the stepped mounds), it is more likely to prevail with a much smaller critical size (a few hundreds of atoms) on a patterned substrate.

Another interesting prediction is that the preferred location for nucleation can be either on the apex or in the valley. This explains the experimental success in directing island nucleation both on top of the mounds or ridges [5–12] and at the bottom of pits and voids [13–15]. The nucleation inside pits and voids has been especially puzzling, because these locations have been thought of as unfavorable sites for strain relaxation. However, our analysis shows that islands can in fact relax strain more effectively in the valley.

The theory shows that the preferred nucleation locations may vary depending on the interplay between strain energy and surface energy. In general, if strain relaxation is dominant, then islands nucleate in the valley; if surface energy is dominant, then islands nucleate in the valley and/or on the apex. These trends may help explain the puzzling effect of buffer layer growth on changing the island location [10]. The Si and/or SiGe buffer layers change the surface energy anisotropy as well as partially relaxing the strain; the detailed balance between these two effects alters the preferred nucleation sites. The high sensitivity of nucleation sites to surface energy anisotropy (see Fig. 3) means that local surface curvature (i.e., step density) can play a critical role in directing island nucleation as experiments [12] have indicated and islands can sometimes nucleate at sidewalls of patterns [9] or at the edges [5,12] where step density is high.

We have focused on nucleation of faceted strained islands. In a classical work by Sholl and Fletcher [24], nucleation of nonfaceted unstrained islands on a patterned substrate was shown to be preferred in the pit using a droplet model. It is interesting to note that for the faceted strained islands the edge energy is usually negligible [19], while for the nonfaceted unstrained islands the edge energy can be significant on a flat surface [18] and its role on a patterned surface needs further attention.

In conclusion, we have developed a theoretical model to elucidate nucleation of strained islands on patterned substrates, based on elastic Green's function method. The theory predicts that island nucleation is generally enhanced on the patterned substrates due to a much smaller critical size and energy barrier reduced by surface curvature effect

and more effective mode of strain relaxation. The interplay of these two factors drives the preferred nucleation sites to vary from the top of an apex to the bottom of a valley, and to the sidewall of a slope. The theory explains the most salient features of the existing experiments. It is suggested that the patterned pits and trenches should be explored further as an effective way to direct island nucleation and self-assembly.

We thank E. Lupton for critical reading of the paper. The work at Utah is supported by DOE-BES program. The work at Beijing is supported by NSFC, the “973” project and CAS.

---

\*fliu@eng.utah.edu

- [1] For a recent collected work, see *Lateral Alignment of Epitaxial Quantum Dots*, edited by O. Schmidt (Springer, New York, 2007).
- [2] S. Yu Shiryayev *et al.*, Phys. Rev. Lett. **78**, 503 (1997); Y. H. Xie *et al.*, Appl. Phys. Lett. **71**, 3567 (1997).
- [3] F. Liu *et al.*, Phys. Rev. Lett. **82**, 2528 (1999); J. Tersoff, C. Teichert, and M. G. Lagally, Phys. Rev. Lett. **76**, 1675 (1996); Q. Xie, A. Madhukar, P. Chen, and N. P. Kobayashi, Phys. Rev. Lett. **75**, 2542 (1995).
- [4] A. H. Li *et al.*, Phys. Rev. Lett. **85**, 5380 (2000).
- [5] T. I. Kamins and R. S. Williams, Appl. Phys. Lett. **71**, 1201 (1997).
- [6] R. Zhang *et al.*, Appl. Phys. Lett. **73**, 505 (1998).
- [7] A. Konkar *et al.*, J. Vac. Sci. Technol. B **16**, 1334 (1998).
- [8] G. Jin *et al.*, Appl. Phys. Lett. **75**, 2752 (1999); G. Jin, J. L. Liu, and K. L. Wang, Appl. Phys. Lett. **76**, 3591 (2000).
- [9] T. Kitajima, B. Liu, and S. R. Leone, Appl. Phys. Lett. **80**, 497 (2002).
- [10] Z. Y. Zhong *et al.*, Appl. Phys. Lett. **82**, 445 (2003); J. Appl. Phys. **93**, 6258 (2003).
- [11] Z. Y. Zhong *et al.*, Appl. Phys. Lett. **82**, 4779 (2003).
- [12] B. Yang, F. Liu, and M. G. Lagally, Phys. Rev. Lett. **92**, 025502 (2004).
- [13] L. Vescan *et al.*, Appl. Phys. Lett. **82**, 3517 (2003).
- [14] Z. Y. Zhong *et al.*, Phys. Rev. Lett. **98**, 176102 (2007).
- [15] A. Pascale, I. Berbezier, A. Ronda, and P. C. Kelires, Phys. Rev. B **77**, 075311 (2008).
- [16] J. Tersoff and F. K. LeGoues, Phys. Rev. Lett. **72**, 3570 (1994).
- [17] V. A. Shchukin *et al.*, Phys. Rev. Lett. **75**, 2968 (1995).
- [18] F. Liu, Phys. Rev. Lett. **89**, 246105 (2002).
- [19] G. H. Lu and F. Liu, Phys. Rev. Lett. **94**, 176103 (2005).
- [20] J. Tersoff, B. J. Spencer, A. Rastelli, and H. von Känel, Phys. Rev. Lett. **89**, 196104 (2002).
- [21] H. Wang, Y. Zhang, and F. Liu, J. Appl. Phys. **104**, 054301 (2008).
- [22] R. V. Kukta, G. Petroff, and D. Kouris, J. Appl. Phys. **97**, 033527 (2005).
- [23] See EPAPS Document No. E-PRLTAO-101-040848 for derivation of a 3D model supplementary material. For more information on EPAPS, see <http://www.aip.org/pubservs/epaps.html>.
- [24] C. A. Sholl and N. H. Fletcher, Acta Metall. **18**, 1083 (1970).